Contrib Mineral Petrol (2003) 145: 600–611
DOI 10.1007/s00410-003-0473-y

ORIGINAL PAPER

Marco Herwegh · Alfons Berger

Differences in grain growth of calcite: a field-based modeling approach

Received: 30 October 2002 / Accepted: 31 March 2003 / Published online: 21 June 2003

Abstract Normal grain growth of calcite was investigated by combining grain size analysis of calcite across the contact aureole of the Adamello pluton, and grain growth modeling based on a thermal model of the surroundings of the pluton. In an unbiased model system, i.e., location dependent variations in temperature-time path, 2/3 and 1/3 of grain growth occurs during pro- and retrograde metamorphism at all locations, respectively. In contrast to this idealized situation, in the field example three groups can be distinguished, which are characterized by variations in their grain size versus temperature relationships: Group I occurs at low temperatures and the grain size remains constant because nano-scale second phase particles of organic origin inhibit grain growth in the calcite aggregates under these conditions. In the presence of an aqueous fluid, these second phases decay at a temperature of about 350 °C enabling the onset of grain growth in calcite. In the following growth period, fluid-enhanced group II and slower group III growth occurs. For group II a continuous and intense grain size increase with T is typical while the grain growth decreases with T for group III. None of the observed trends correlate with experimentally based grain growth kinetics, probably due to differences between nature and experiment which have not yet been investigated (e.g., porosity, second phases). Therefore, grain growth modeling was used to iteratively improve the correlation between measured and modeled grain sizes by optimizing activation energy (Q), pre-exponential factor (k_0) and grain size exponent (n). For $n = 2$, Q of 350 kJ/mol, k_0 of 1.7×10^{21} $\mu m^n\ s^{-1}$ and Q of 35 kJ/mol, k_0 of 2.5×10^{-5} $\mu m^n\ s^{-1}$ were obtained for group II and III, respectively. With respect to future work, field-data based grain growth modeling might be a promising tool for investigating the influences of secondary effects like porosity and second phases on grain growth in nature, and to unravel differences between nature and experiment.

M. Herwegh (✉) · A. Berger
Institute of Geological Sciences, University of Bern,
Baltzerstr. 1–3, 3012 Bern, Switzerland
E-mail: herwegh@geo.unibe.ch
Tel.: +41-31-6318764
Fax: +41-316314843

Editorial responsibility: J. Hoefs

Introduction

Grain growth is one of the most fundamental metamorphic processes and occurs over a wide range of temperatures, i.e., diagenesis up to ultra-high temperature, in all rock types (e.g., Spry 1969). In this sense, grain size is a key parameter for deformation mechanisms, diffusion kinetics and transport properties of rocks. In order to gain insights into the kinetics of grain growth, numerous experiments have been performed on various mineral aggregates such as calcite, quartz and olivine (e.g., Chai 1974; Tullis and Yund 1982; Karato and Masuda 1989; Nichols and Mackwell 1991; Covey-Crump 1997; Masuda et al. 1997; Freund et al. 2001). These experiments are consistent with findings derived from material sciences, which indicate that grain size, temperature and time are related via an Arrhenius-type equation:

$$(D^n - D_0^n) = k_0 \exp^{(-Q/RT)}(t - t_o) \quad (1)$$

where D is the final grain size at time t, and D_o is the initial grain size at time t_o, k_0 is a pre-exponential factor, Q is the activation energy, and T is the temperature in Kelvin. Theoretical treatments of grain growth yield grain size exponents n of 2, 3, or 4 but in experiments n values over a larger range are observed because n depends on a variety of parameters such as, for example, on the purity of the samples and mechanisms involved in the grain growth (see e.g., Brook 1976; Covey-Crump 1997; Evans et al. 2001). To apply an experimentally derived grain growth law to nature, several points require special attention. (1) In contrast to experimental approaches, where the temperatures are held constant

during the entire interval of the experiment, temperature continuously varies in nature as a function of geologic evolution. Therefore, the T–t path has to be accurately known before a grain growth law can be applied to natural samples (Joesten 1983, 1991; Joesten and van Horn 1999). (2) Related to changes in P and T, extrinsic and intrinsic properties of a rock can change and therefore influence grain growth (e.g., dehydration reactions). In this sense, it is crucial to know what the critical parameters are and at which time and to what extent they will affect grain growth. (3) Furthermore, several parameters like second-phase minerals, chemical impurities, fluids, chemical potentials and strain energy drastically influence the grain growth behavior (e.g., Brook 1976; Evans et al. 2001) and can therefore induce considerable deviations. When considering grain growth in nature the following questions need to be addressed:

- What is the T–t path in the area of interest?
- What is the grain size evolution on the pro- and retrograde temperature path and are there potential deviations related to changes in the rock properties?
- What are the major parameters that influence grain growth kinetics in nature?

In order to answer these questions, grain growth in nature within a simple geological framework should be investigated, where the T–t paths are well defined, the rocks are nominally pure and other processes such as deformation or mineral reactions can be excluded. For this purpose, we studied a contact metamorphic marble from the Adamello massif (northern Italy). A description of the geological framework and characterizations of the samples investigated are presented at the beginning of this work. Based on a well-known geological setting, thermal models are developed and their suitability is discussed. In the second part, the chosen T–t path is used together with experimental parameters to model a theoretical grain size evolution. Finally, we compare the modeled results with those observed, and discuss the relevance of nature-based grain growth laws.

Geological setting

The area investigated comprises undeformed, subhorizontal Permo-Mesozoic sediments, which were deposited on the crystalline basement of the Southern Alps (Fig. 1; see also Callegari et al. 1999). These sediments are intruded by the Monte Re di Castello tonalite, which is part of the Adamello plutonic suite (Calleghari et al. 1999). The Monte Re di Castello tonalite sensu stricto is interfingered with a granodiorite, which is of similar age (40–42 Ma, Hansmann and Oberli 1991). This suite of intrusions caused pronounced contact metamorphism of the entire sedimentary sequence (e.g., Riklin 1983; Brack 1984). The samples studied in this work are from the Calcare di Dosso dei Morti, which represent former stromatoporoid reefs and laterally pass into the more lagoonal facies of the Calcare di Angolo (Fig. 1). In case of the Calcare di Dosso dei Morti, contact metamorphism induced a continuous transition from fine-grained non-metamorphic platform carbonates to coarse-grained calcite marbles (Schmid 1997). Pre-intrusion temperatures were estimated at 200 °C (Riklin 1983) and peak metamorphic temperatures were approximately

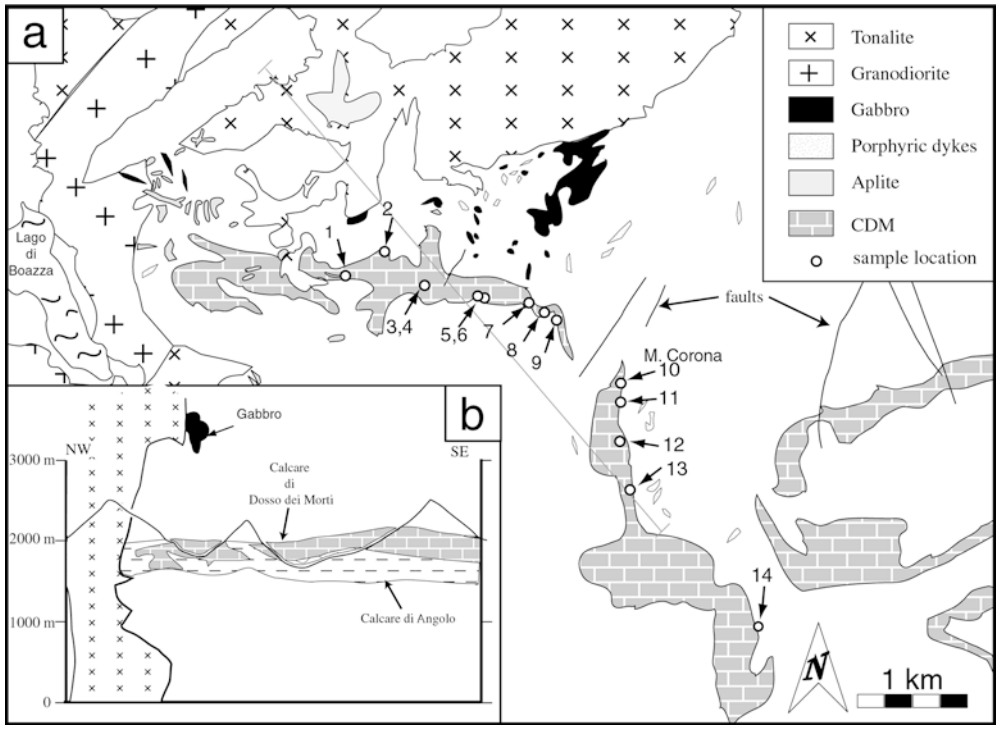

Fig. 1 **a** Geological map showing the trace of the section investigated and sample locations. **b** Cross section of the geologic situation

600–650 °C at the contact (Riklin 1983). In sum, the geological framework is sufficiently simple to provide a well-constrained *T*–*t* path and therefore can be used as a natural laboratory to investigate the grain growth behavior of carbonate rocks.

Sample description and grain size analysis

As evident from the constructed cross section in Fig. 1b, the contact of the intrusion is vertical and therefore there is a 1:1 correspondence between map distance from the contact and true distance. The Calcare di Dosso dei Morti show an increasing grain size as the contact of the intrusion is approached (Figs. 2, 3, Table 1) accompanied by a change in color from predominantly gray to white. The color change is attributed to small-sized second phase particles of former organic material, which decayed and became mobilized with increasing temperature (Schmid and Flammer 2002). Two kilometers away from the contact, the grain sizes of the limestones appear to be unaffected by the contact metamorphism and are therefore interpreted to represent the starting material of the natural grain growth experiment.

To investigate the temperature-dependent grain size change in a quantitative manner, samples were collected at various distances from the intrusion contact (Fig. 1). Ordinary rock chips were prepared for microstructural characterization. Due to considerable changes in grain size, which range from micron to centimeter scale, grain boundary outlines were traced from: (1) SEM images of polished rock chips that were previously treated with two-step etching for fine grain sizes (< 40 μm, see Herwegh 2000), (2) images of thin section micrographs for intermediate grain size ranges (40–1,000 μm), and (3) images of polished and then scanned hand specimen for coarse-grained samples (> 1,000 μm). Based on the resulting grain boundary outlines, a macro in Image SXM (Version 1.61) was used to calculate linear intercept grain sizes (e.g., Exner 1972). In this way, two patterns consisting of parallel vertical and horizontal lines were superposed on the grain boundary maps to calculate the lengths of the resulting intercepts. Before final analysis, tests with respect to the reproducibility of the results using different line spacing were performed. The results indicate that spacing is not critical as long as a statistically sufficient number of grains is analyzed. We used an average pattern spacing of approximately 0.3–0.5 times the average grain size. The prepared samples represent only sections through three-dimensional aggregates inducing truncation effects. As a consequence of sectioning the real 3-D grain size is underestimated because only a small number of section

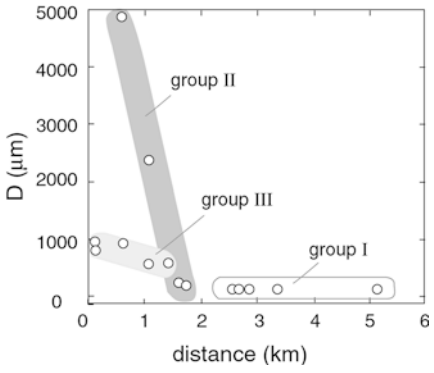

Fig. 3 Relationship between distance from the pluton and calcite grain size. Three different groups can be recognized

Table 1 Sample list with constructed distance from the pluton (see Fig. 1), average grain size (D) estimated by the linear intercept method and used number of grains for the evaluation of D. Given temperature is taken from maximal temperature from model A-5

Sample	Distance (m)	T_{max} (°C)	D (μm)	No. of grains
1	100	627	832	127
2	125	622	669	154
3	600	485	800	154
4	600	485	4,834	225
5	1,050	414	440	415
6	1,050	414	2,357	235
7	1,415	376	466	181
8	1,600	359	115	158
9	1,725	349	66	181
10	2,550	304	7	228
11	2,650	300	5.4	209
12	2,850	296	5.7	223
13	3,350	284	6.4	369
14	5,100		2.7	206

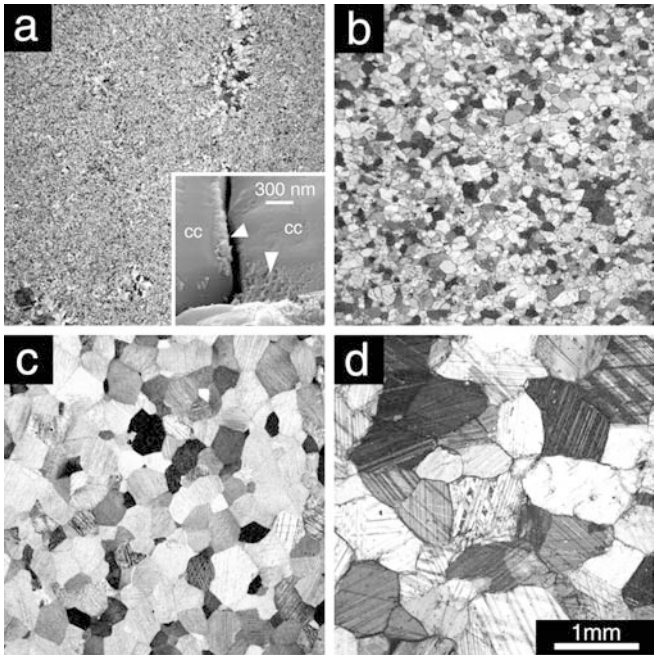

Fig. 2a–d Thin section micrographs of samples from di Calcare dei Dossi di Morti with decreasing distance to the pluton: **a** sample 10 (2,550 m), **b** sample 9 (1,725 m), **c** sample 8 (1,600 m) and **d** sample 7 (1,415 m). Scale bar valid for all images. Note the coarser grained patches in sample 10. The *inset* in **a** represents a high-resolution FEG image showing nano-scale flakes of organic matter accumulated at triple junctions of calcite (*cc*) grains

cuts represent the true sphere diameter (e.g., Exner 1972). Different approaches exist for the extrapolation of 2-D to 3-D grain sizes, which are mostly based on simplified assumptions about the grain shape. For grain growth investigations, 2-D grain sizes are sufficient, particularly when the results are compared with experimental data analyzed in a similar manner. Therefore, no correction was applied to account for truncation effects (Table 1).

The starting material generally consists of a very fine-grained matrix (5 μm) locally containing small patches of coarse-grained calcite (Fig. 2a). It is important to note that in the low-T region, the fine-grained areas were chosen exclusively for grain size analyses. Basically, three different groups can be distinguished (Fig. 3).

Group I occurs at distances from the pluton larger than 2 km. There, the grain size is constantly small ranging from 3–7 μm. A characteristic feature of group I is the gray appearance, which primarily is attributed to the occurrence of organic matter (see also Schmid and Flammer 2002). Detailed high-resolution investigation using a SEM (Jeol JSM-6300F) with field emission gun reveals that the organic matter exists as flakes with diameters of about 25 nm and preferentially is accumulated at triple junctions of calcite grain boundaries (see inset in Fig. 2a).

In contrast, groups II and III have a white appearance. Furthermore, in both groups grain sizes increase with temperature but the grain size increase is more pronounced in group II than in III (Fig. 3). In this context, it is important to note that group II and III grains can occur within the same outcrop. The grain boundaries of calcite grains generally are straight to slightly curved ending typically at triple junctions of 120 ° (Fig. 2). Chemical analysis performed by Schmid (1997) showed that the samples contain ≥99 wt% carbonate minerals. Minor amounts of dolomite are found in a few low temperature samples (0–4 wt%) and < 1 wt% of silicate, Fe-oxides and Fe-sulfides are present. In particular in coarse-grained samples of groups II and III, twinning is a common feature (see Fig. 2). These twins are thin, straight-sided with no evidence of high temperature phenomena like twin boundary migration (cf. Burkhard 1993) and so the twinning is interpreted as having occurred during a late stage of the exhumation and that any influence on grain growth can be neglected.

In terms of the transition from group I to II/III, the change in appearance from gray to white is attributed to a decomposition of the organic matter (see also Schmid and Flammer 2002). In other words, the nano-scale flakes must decay, most likely into CO_2 and CH_4, a process that requires the presence of an aqueous fluid. Fluid presence is particularly evident in some outcrops in the transition zone where irregularly shaped white bands with diffuse contacts dissect the gray limestone (Fig. 4). As a consequence of their shapes, veins can be excluded and therefore the only remaining possibility is a fluid-induced transformation of the host rock. Interestingly, the average grain size and the distribution width are larger in the fluid affected band than in the gray host rock (grains size distribution diagrams in Fig. 4).

Temperature evolution in the contact metamorphic aureole

Temperature constraints

The initial temperature in the wall rock can be calculated by combining an assumed thermal gradient with the

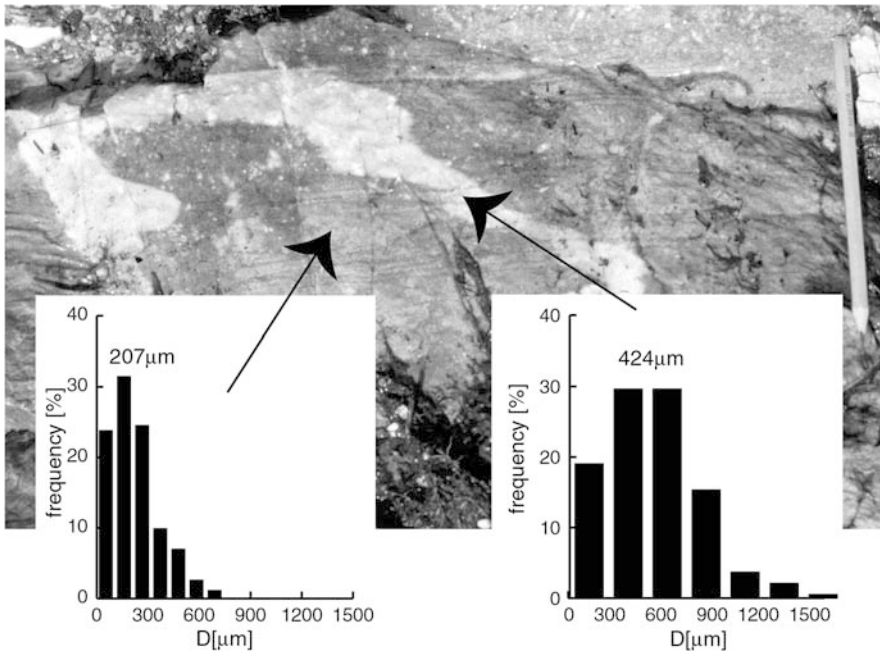

Fig. 4 Original gray limestone dissected by a curved and irregularly shaped white band. Note that both gray and white parts consist completely of calcite and that the sedimentary layering in the limestone is horizontal. *Insets* show the grain size distribution diagrams for both white and gray parts

known overburden of 6.5-km sediments (Callegari 1962; Riklin 1983; Matile and Widmer 1993) resulting in 130 or 180 °C with geotherms of 20 and 28 °C/km, respectively. Illite crystallinity data indicate an chi- to epi-metamorphic conditions at a distance of 2 km away from the contact (Riklin 1983), which may be slightly influenced by the heat of the pluton.

Bucher (1982) investigated a thermal gradient perpendicular to the contact aureole in the area of La Uzza in silicic dolomites where the ''Forsterite in'' and the ''Tremolite out'' isograd correlates with peak temperatures of approximately 525 and 400 °C, respectively (see Fig. 12 in Gerdes et al. 1999; Bucher 1982). However, the distance of the isograds to the present day border of the pluton varies. A thermal gradient of 315 °C/km results for distances of 400–800 m.

Thermal modeling

Thermal evolution around magmatic bodies has been intensively investigated (e.g., Jaeger 1964; Hanson and Barton 1989; Turcotte and Schubert 2002). The heat flow equation cannot be solved analytically and numerical modeling is required to gain insights into a thermal history. In this respect, the size and shape of the magmatic body, the magma temperature and the initial country rock temperature are the most important input parameters for thermal modeling (e.g., Jaeger 1964; Davidson et al. 1992). We modeled the thermal evolution of the area under investigation using the heterogeneous heat flow program HEAT (KWare, programmed by K. Wohletz; University of California). A comprehensive treatise on the physical background and the numerical solution to the heat flow equation are given by Turcotte and Schubert (2002). Table 2 presents the parameters chosen to model heat flow by conduction. In addition, we checked for potential deviations from the obtained results by convective heat flow, a scenario that might occur for example during fluid flow. However, applying permeabilities characteristic for limestones (Hanson 1995), convective heat flow has only a very limited influence on T-history and can therefore be neglected.

Our model used an overburden of 4 km and a thermal gradient of 28 °C, into which a pluton with a diameter of 4 km is intruded (Fig. 5a). Note that the thinner overburden of the model (4 km instead of 6 km) was compensated for by an enhanced surface temperature (Table 3). This situation represents a good approximation

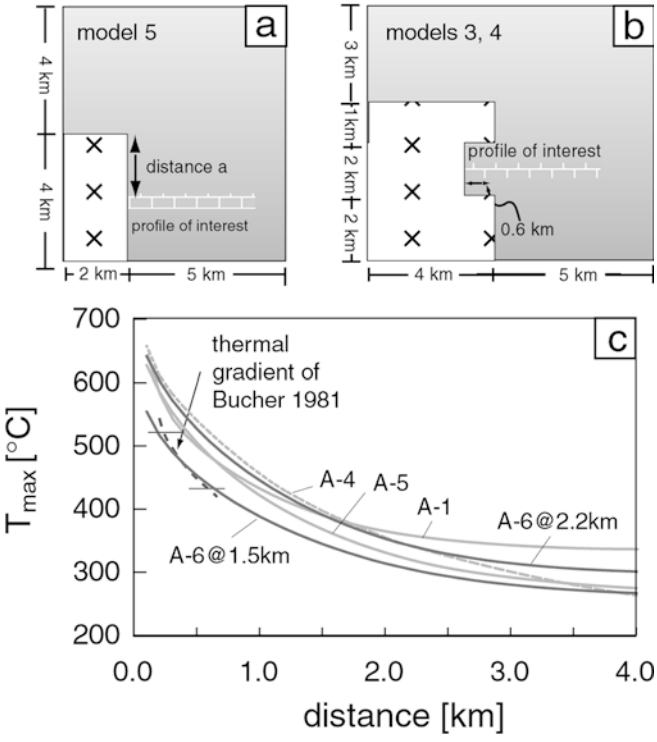

Fig. 5a–c Schematic drawing of the two main thermal models. **a** Model A-5 with box-shaped pluton geometry. The distance between top of the pluton and the investigated profile is indicated (distance a). **b** Models A-3 and A-4 with irregular shapes. **c** Maximum temperature as a function of distance from the pluton for different models. Temperature constraints from mineral assemblages are also indicated (Bucher 1981)

to our example of the Monte Re di Castello pluton (see geological setting and Fig. 1) and therefore provides a characteristic *T–t* path for the metamorphosed Calcare di Dossi dei Morti (Fig. 6a, inset). In order to study the sensitivity of the *T–t* curve to different country rock temperatures and shapes of the pluton, we calculated a series of thermal models (Tables 2 and 3; Fig. 5). The resulting T_{max} curves show little variation but these variations are somewhat more pronounced close to the contact. Besides slight differences in T_{max}, the models also show variations in the *T–t* path, a fact that has to be considered with respect to the later grain growth modeling. In this sense, major temperature variations can exist near the edges of the pluton, because there, heat dispersion occurs in two directions. The modeling results of the thermal evolution around complex shaped plutons (models A-3 and A-4; Table 3; Fig. 5) show the same variations in temperature evolution as box-shaped models

Table 2 Physical parameters used for thermal modeling

Model	A-1	A-2 toA-6
K country rock ($Wm^{-1}K^{-1}$)	1.3	1.9
ρ (kg m^{-3})	2,500	2,500
Heat magma (°C)	900	900
K magma (Wm^{-1} K^{-1})	3.7	3.7
Grid size (km)	0.1	0.1

Table 3 Model dimensions and time constraints

model	half-width [km]	size pluton [km^2]	shape	surface T of model [°C]	remark	run time [Ma]	size model [km]
A-1	3	12	□	70		1.2	8x7
A-2	3	9	□	40	const. T <3 ka	0.63	8x7
A-3	4 (-0.6)	10.8	⊏	90		1	8x9
A-4	4 (-0.6)	10.8	⊏	30		0.3	8x9
A-5	2	8	□	30		1.06	8x7
A-6	2+	10.2	▱	30		0.63	8x7

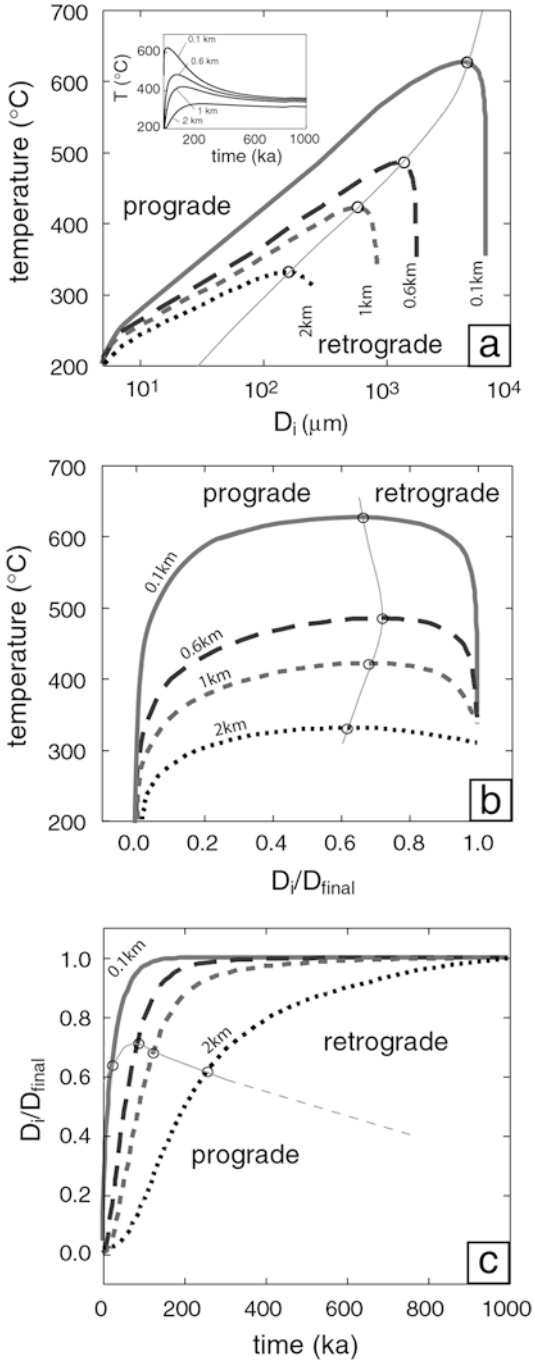

Fig. 6a–c Influence of pro- and retrograde temperature evolution on grain growth. **a** and **b** show temperature versus modeled grain size (D_i) and normalized grain size (D_i/D_{final}), respectively. **c** Evolution of the normalized grain size with time. *Inset* in **a** represents typical *T–t* paths for model A-5 at different distances from the pluton contact

at their top. Besides these variations in the close vicinity of irregularities in pluton shapes, however, all calculated *T–t* paths are rather similar in comparison to our main box-shaped model. Therefore, large-scale bulges or irregularities (kilometer-sized) may affect the *T–t* path only to a minor extent, and even then only close to the edges. Due to the stability of the thermal modeling, and only small variations between the different models, we selected model A-5 for further calculations because it comes closest to the temperature constraints at the pluton contact and the country rock far from the intrusion mentioned above.

Grain growth modeling

Calculating the expected grain sizes

Experimental *T–t* paths differ significantly from natural ones in that the time interval of peak metamorphism and heating and cooling periods vary as a function of time. Hence, in nature, the time-dependent temperature evolution has to be known in order to investigate the grain growth kinetics (see also Joesten 1991) resulting in a grain growth law in form of:

$$\frac{dD}{dt} = \frac{D^n - D_0^n}{nD^{n-1}} \left(\frac{1}{t - t_0} + \frac{Q}{RT^2} \frac{dT}{dt} \right) \tag{2}$$

In this equation T and t are related to each other via the function $f_{(t)}$. As mentioned in the previous section, however, this function results from numerical solution of the heat flow equation. As a consequence, a numerical approach is also required for Eq. (2). This is achieved by calculating iteratively the changes of a starting grain size D_o for time intervals (i) with specific temperatures (T_i). The final grain size to be expected is therefore:

$$D_i = D_0^n + \sum_{i=o}^{N} \left(k_o \cdot \exp^{\left(-Q/RT_i\right)} \cdot (t_i - t_{i-1}) \right)^{1/n} \tag{3}$$

where N is the number of time steps. Note that this equation can only be solved when the *T–t* path is known, i.e., modeled as shown in the previous section. To calculate D_i, the required variables Q, k_o and n can either be taken from experimental investigations or, as will be demonstrated below, be derived by modeling the trends defined by the field data.

Influence of the *T–t* path on grain size

In this section, we will quantify the influence of the *T–t* path on grain growth as a function of variable distances from the pluton contact. In contrast to the isothermal growth law [Eq. (1], the sequential law [Eq. (3] allows the examination of grain growth during prograde, peak and retrograde T evolution. For this purpose, experimental values of Covey-Crump (1997, $Q = 173.6$ kJ/mol, $n = 3$ and $k_o = 2.5 \times 10^9$ μm^n s^{-1}), a starting grain size of 5 μm and the temperature model A-5 were chosen to calculate the grain size evolution at 0.1, 0.6, 1 and 2 km distance from the pluton wall-rock contact. In order to compare the amount of grain growth during pro- and retrograde stages, the grain size was normalized by:

$$D_{norm} = D_i / D_{final} \quad (4)$$

where D_i is the modeled grain size at t_i and T_i and D_{final} the final grain size. Based on the modeling results we emphasize the following points: (1) grain growth takes place at all locations even at distances 2 km away from the contact (Fig. 6a); (2) although the major part of grain growth occurs during prograde metamorphism, a considerable amount (30–40%) of the entire grain size increase is generated during the retrograde temperature path (Fig. 6b); (3) grain growth is highly heterochronous because samples near the contact (e.g., 100 m) reach grain sizes close to the final value at an early stage while samples far away from the contact grow over a much longer time period (Fig. 6c); (4) in all samples, prograde grain size increases take place over shorter time intervals than the retrograde one (Fig. 6c). Note that these results are of a general character that is independent of the selected Q, n and k_o values.

In addition, the influence of a fast (model A-5) and slow cooling (model A-1) path on the overall grain size evolution was investigated. Note that peak temperature is nearly identical for both models. At a constant distance of 600 m from the contact, the grain size increase is faster in model A-5. However, the final grain size is larger in the slow cooling model A-1. This general trend is consistent for all final grain sizes undergoing a slow cooling path but the final grain sizes of the slow cooling model converge with those of the fast cooling model at high temperatures (Fig. 7). Hence, slight departures due to differences in the T–t path have to be taken into consideration. In summary, both the time-dependent changes in T and the distance of the point of interest from the pluton contact influence the grain size evolution and therefore, the final grain size.

Relevance of the analyzed grain sizes for normal grain growth

Thermal modeling, locally constraint by nature-based peak temperature estimations, provides a T–t path allowing the extraction of maximum temperatures for each locality in the metamorphic aureole. These data are used in Eq. (3) to model normal grain growth in the Calcare di Dossi dei Morti. The relations between grain size and temperature can be best shown by using the maximum temperatures at each locality from the thermal model and the measured grain size (Fig. 8). As already shown in the distance versus temperature diagram, three different groups can be identified (cf. Figs. 3, 8). As a consequence of the asymptotic shape of the P–T path at distances far from the pluton contact, group I samples show only small differences in peak temperature ranging from 280–310 °C, which is somewhat higher than the inferred pre-intrusion temperature. For the purpose of grain size modeling, these rocks will be taken as starting material. The different trends of group II and group III observed in Figs. 8 and 9 will be discussed in the following sections.

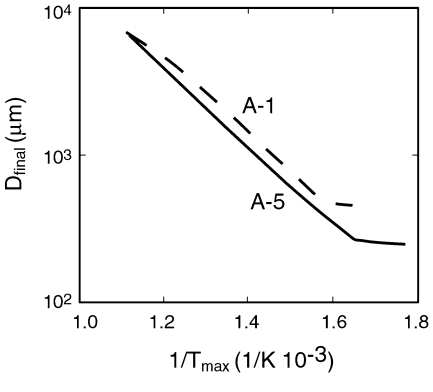

Fig. 7 Differences in final grain size between models A-1 and A-5 as a function of the $1/T_{max}$ at 600 m

Applying experimentally derived parameters to nature

Although a large variety of grain growth experiments have been performed on calcite aggregates (Chai 1974; Tullis and Yund 1982; Covey-Crump 1986, 1997; Olgaard and Evans 1986, 1988; Freund et al. 2001; Renner et al. 2002), only few studies exist (e.g., see Table 1 in Joesten 1991; Covey-Crump 1986, 1997; Freund et al. 2001) where all parameters were determined, i.e., Q, k_0 and n, required to apply an experimental grain growth law to nature (Table 4). These experimentally derived values reveal variations in Q between 60–232 kJ/mol, in k_o between 3×10^2 and 1×10^{11} $\mu m^n/s$ (based on different n) and in n between 2 and 3. Modeled grain sizes were obtained by using Eq. (3), the T–t paths of model A-5 and experimental parameters of Table 4. None of the modeled trends fits the estimated temperature dependence of the natural samples (Fig. 8) and the following points need to

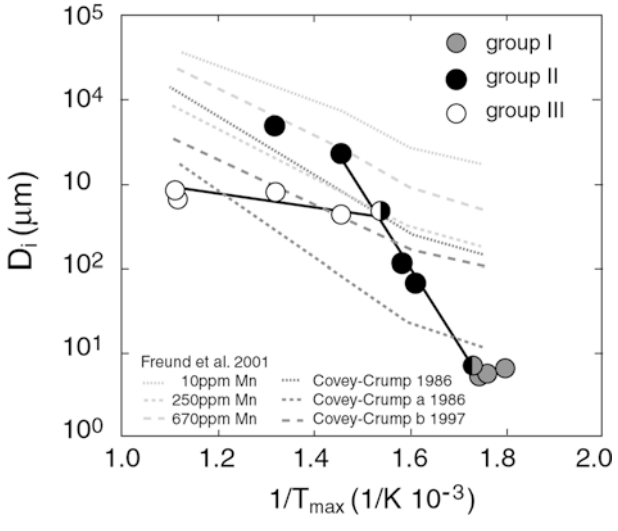

Fig. 8 Modeled grain sizes using temperature from model A-5 and experimentally derived grain growth kinetics. Measured natural data are given for comparison

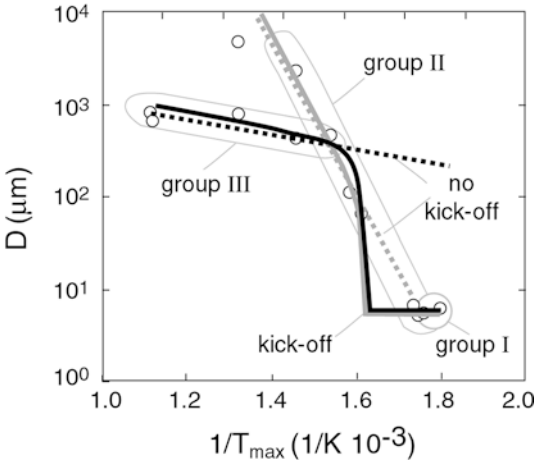

Fig. 9 Relationship between inverse T from model A-5 and measured grain size of the different groups (*D*). Modeled grain size trends for group II (*gray*) and III (*black*), with (*solid*) and without (*stippled*) kick-off temperature for calcite grain growth

be emphasized: (1) all of the field observations cannot be described using one set of experimentally derived parameters in Eq. (3); (2) assuming group III to be representative of the general grain size trend, it is not possible to connect these data with group I (starting material); (3) taking group II as a major trend and extrapolating it towards higher T, unrealistically large grain sizes would be expected at the pluton's contact (Figs. 3, 8). Consequently, we postulate two different growth behaviors, which cannot be described by existing experimental parameters. These different growth behaviors might be attributed to the complicated influence of other factors not explicitly investigated in the experiments (e.g., second phases, solute impurities, etc.) and/or the extrapolation of laboratory experiments to nature. On the other hand, we have to take into account that grain growth ceased in some of the natural samples due to boundary pinning by second phase particles or differences in solute concentrations (see also Olgaard and Evans 1988; Covey-Crump 1997). For dry experiments, for example, Covey-Crump (1997) suggested that differences in the pore distribution induce different rate-controlling processes and therefore affect the growth regimes in calcite. An extensive treatise with this respect is out of the scope of this study and will be presented elsewhere. In light of the differences between group II and III growth behavior, we can list at this stage the following facts: (1) in the samples investigated there exist variations in the Sr and Mn contents. For the latter, experiments of Freund et al. (2001) suggest that Mn can enhance the growth rate of calcite. However, none of the observed chemical variations in nature correlate with our grain size trends and are therefore considered to be of secondary importance only; (2) samples 3 and 4 are from the same outcrop and show small and large grain sizes, respectively, but they are characterized by similar type, quantity and size of second phases. Grain boundary pinning by second phases can therefore not account for the difference in grain size between the two groups; (3) variations in starting grain size, as is the case for the micritic and sparitic parts of the limestones, might also affect the final grain size (Fig. 2). However, we modeled the final grain sizes using starting grain sizes of 5 and 500 μm. In case of sample pairs 3/4 and 5/6, which are from the same outcrop but show maximum grain size variations, the modeling suggests grain size differences of factors of 1.25 and 1.4, respectively, compared to 6 and 5 as actually observed ones. Variations in the starting grain size alone cannot therefore explain the observed grain size differences between groups II and III. In addition, the spatial distribution of group II in the field is too large to be attributed to a subordinate number of sparitic patches observed in the original limestones.

To conclude this section, extrapolation of experimentally derived grain growth kinetics works well for small-scale structures in nature, which have seen *T–t* conditions similar to those used in experiments (e.g., Joesten 1991; Joesten and van Horn 1999) but becomes more problematic when extrapolations towards lower temperatures and long-term intervals in natural situations are required. For the present case study, two different sets of kinetic parameters are required to describe group II and III grain growth behavior.

Natural constraints used as input parameters for modeling

To reduce the misfit between observed and modeled grain sizes based on experimental parameters, an

Table 4 Experimentally estimated constants for normal grain growth of calcite aggregates

Study	*n*	Q (kJ/mol)	ko ($\mu m^n/s$)
Freund et al. (2001) (10 ppm of Mn)	2	99	3.00E+02
Freund et al. (2001) (250 ppm of Mn)	2.4	165	1.26E+07
Freund et al. (2001) (670 ppm of Mn)	2.3	147	3.15E+06
Covey Crump (1986)	3	174	2.50E+09
Covey-Crump (1997), data of Olgaard and Evans (1986, 1988)	3	232	1.22E+11
Covey-Crump (1997)	3	162.6	5.94E+07
This study (group II)	2	350	1.7E+21
This study (group II)	3	525	1.6E+38
This study (group III)	2	35	2.5E−05
This study (group III)	3	50	1.0E−01

optimization of the latter is required. This can be done by changing n, Q, and k_o.

With respect to n, nature gives no indication about the appropriate value. However, experiments investigating calcite grain growth generally show values of n between 2 and 3 (e.g., Chai 1974; Tullis and Yund 1982; Olgaard and Evans 1986; Covey-Crump 1997; Freund et al. 2001). As a first step, we therefore used one of them, arbitrarily selected a value for Q and optimized k_0 for the chosen Q. For the optimized parameters, the ratio (R) of the modeled grain size divided by the measured grain size was calculated for each data point. Note that modeling was carried out separately on data of group II and III. Within one group, the mean and standard deviations of the obtained R values were taken, and then k_0 was iteratively changed until the mean of R was equal to 1. At this stage, Q, k_o and the standard deviation in R were stored and the procedure was repeated for a suitable series of Q values, first keeping the same n value, and then using the alternative n in a second modeling series. To choose those Q and k_o values most reliable for a specific n, Q was plotted versus the standard deviation of R allowing the selection of the parameters with the lowest standard deviation for each n (Fig. 10).

Based on the modeling results, for all chosen values of Q, the grain sizes at large distance from the pluton contact are increasing too much (Fig. 9). Thus, the model allows grain growth at lower temperatures than actually occur in the natural example. This apparent discrepancy can be eliminated by introducing a kick-off temperature, i.e., a temperature value below which grain growth is prevented. In practice, this is achieved by starting the grain growth iterations of Eq. (3) only when the temperature is higher than the selected value (Fig. 9). The existence of a kick-off temperature for grain growth suggests a sudden change in the growth behavior of calcite, which can either be due to an intrinsically controlled change in the growth kinetics or to an externally controlled parameter. The fact that the aforementioned change in color coincides with the transition of group I to III, i.e., with the onset of pronounced grain growth, implies that the retardation temperature is linked with the decay of the nano-scale second phase particles of organic origin. Before their decomposition, they prevented grain growth because they pin the calcite grain boundaries (see inset in Fig. 2a; see also Oertel 1983; Olgaard and Evans 1988; Walker et al. 1990; Dresen et al. 1998; Herwegh and Kunze 2002). Compared to a pure system, this behavior results in smaller calcite grain sizes, which persist as long as pinning continuous. For the modeling approach, the appropriate kick-off temperature for calcite grain growth must be situated somewhere in the temperature range between 310 and 350 °C (Fig. 9). As demonstrated above, the decay of the organic matter must have been related to aqueous fluids (Fig. 4). Recently, Akinfiev and Diamond (2002) suggested that the log K value for the reaction graphite $+ H_2O = CO_2 + CH_4$ becomes larger than 0 at

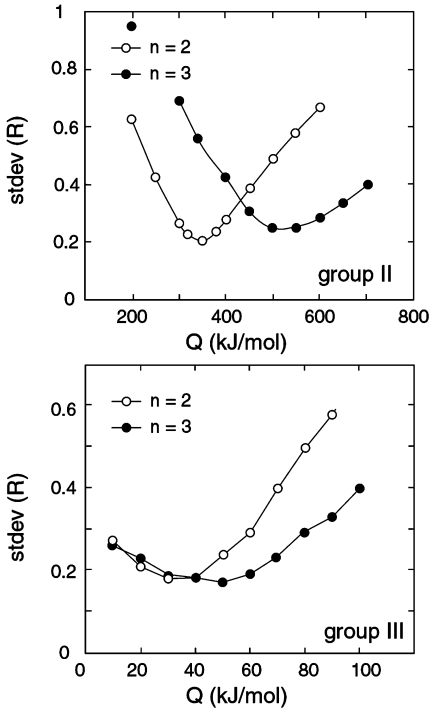

Fig. 10 Estimation of Q, n and k_o. Diagrams show Q values vs. standard deviation of the ratio ($R = D_{mod}/D_{meas}$). Q values with minimized standard deviation are used for the corresponding n

temperatures of 350 °C. For these reasons we chose a Kick-off temperature of 350 °C, yielding results with a good correlation between modeled grain sizes and those measured in nature (Fig. 9). The physical reason for the drastic grain size increase directly above the kick-off temperature, is the enhanced grain boundary velocity, because the grain sizes are too small compared to grain growth in a pure system. This can be demonstrated using Hillert's (1965) approximation, which expresses the net driving force (F) acting on a particular grain boundary

$$F = 2C\gamma\left(\frac{1}{D_c} - \frac{1}{D}\right) \tag{5}$$

where C is a factor that relates to the grain boundary curvature, γ is the surface energy, D_c is the critical grain size below which grains will shrink and D is the measured grain size. In our case, $D \gg D_c$ but because of the grain size stabilization, D is about 60 times smaller than it would be in a pure system at the corresponding temperature. As long as grain size stabilization persists, F will continuously increase. In addition, the velocity (V) of the migrating grain boundary is defined by

$$V = MF \tag{6}$$

where M is the grain boundary mobility, which is inversely related to temperature (e.g., see Eq. (10) in Evans et al. 2001). Because of the small grain size after the decay of the second phases, the driving force (F) will be high, whereas M changes only slightly (factor 1.15) in the temperature range between 1.7 and 1.8 K^{-1} (Fig. 9).

In other words, V will increase with F at similar M, inducing rapid grain growth per time interval. During the following growth period, V will continuously decrease approaching values of the nano-scale particle unaffected growth behavior. As a consequence, final grain sizes close to the Kick-off temperature, i.e., grains whose growth interval was short during their pro- and retrograde path (see Fig. 6), will induce a steep slope in $1/T$ versus D diagram (Fig. 9). Similar retardation effects with respect to the onset of grain growth can occur in experimental investigations, for example, by rearrangement of pore distributions or intervals of primary recrystallization (e.g., Olgaard and Evans 1988; Covey-Crump 1997). In those particular cases, careful detection of the onset of normal grain growth (t_0) is required to obtain proper kinetic parameters (see Covey-Crump 1997).

Applying the implemented kick-off term of grain growth and the modeling approach described above for group II, Q values of 350 and 525 kJ/mol and k_0 values of 1.7×10^{21} and 1.6×10^{38} $\mu m^n\ s^{-1}$ are determined for n of 2 and 3, respectively, (see Fig. 10, Table 4). For $n=2$, the standard deviation is slightly smaller than for 3. In addition, 350 kJ/mol is within the range of experimentally derived activation energies of Ca, C and O self-diffusion in calcite (see for example compilation in Renner and Evans 2002) while 525 kJ/mol is much larger than any experimentally derived value. For these reasons, we favor the obtained parameters related to n equal to 2. In case of group III the activation energies for both n equal to 2 and 3 are between 35–50 kJ/mol, and therefore are very similar. This implies that a choice of n between 2 and 3 is of subordinate importance for group III grain growth. These Q values are situated in the lower region of the experimentally determined activation energies for calcite grain growth (see Table 1 in Joesten 1991). On the other hand, such values are far away from activation energies typically observed for diffusion processes (see compilation in Renner and Evans 2002).

When comparing natural data with grain growth experiments, it is noteworthy that: (1) most experimental results are influenced by remaining porosity (e.g., Olgaard and Evans 1988; Covey-Crump 1997) and might not represent grain growth kinetics of a pure and pore free material; (2) experimental durations of grain growth investigation range between minutes and months, resulting in grain size changes of approximately one order of magnitude (e.g., Covey-Crump 1997; Freund et al. 2001; Renner et al. 2002). In our natural case, however, the time span available for grain growth is 1 million years, the grain size change covers 3 orders of magnitude and the temperatures are a couple of hundred degrees centigrade below experimental conditions. (3) Experiments carried out on wet calcite or calcite (Tullis and Yund 1982; Covey-Crump 1997), (Renner et al. 2002 and references therein) show that fluid can enhance the growth rate, particularly when present as thin films along grain boundaries, and is not affected by dragging of pores. Based on these considerations, we believe that at least group II grains represent a second phase unaffected growth behavior, which probably was accelerated by the presence of fluids.

Several remarks with respect to our obtained parameters are required: Q and k_0 values are only valid if the processes involved in grain growth were continuously active over the entire period of time. This point is particularly questionable in light of the fluid enhanced growth behavior of group II. As mentioned above, grain sizes would become unrealistically large when using the obtained grain growth kinetics towards the contact. Additional parameters like time restrictions on fluid activity or pinning by second phase particles might be responsible for the observed discrepancy. Based on the argument presented above, we can exclude second phases to be responsible for the differences between group II and III, but we cannot exclude the fact that second phases influence both group II and III in a similar manner. If this were the case, second phase pinning would have to occur at larger grain sizes for group II than for group III.

To summarize this section, natural calcite aggregates always contain a certain degree of impurities. In the best case, these impurities are small and homogeneously distributed and therefore, their effect on the normal grain growth behavior of a mineral is minimized. Nevertheless, at low temperatures, the impurities will pin the grain boundaries because the grain boundary mobility is too low. As soon as temperature rises and the impurities become mobilized, fast grain growth becomes possible, but only until the remaining impurities start to affect the grain growth behavior again. Therefore, in a natural environment, only a small T window exists in which grain growth of a pure system can be investigated.

Concluding remarks

The combination of field-based thermal and grain growth modeling proved to be a suitable approach to estimate parameters required for the description of grain growth kinetics in contact metamorphic aureoles. In addition, grain growth in the natural example occurred at relatively low T, over long t intervals and induced grain size changes over several orders of magnitude, i.e., all conditions that cannot be reached within reasonable time-frames in experimental investigations. The study demonstrates that mineral reactions, for example, the fluid induced decay of organic matter, can have a drastic influence on grain growth and needs to be considered when extrapolating experiments to nature.

The measured grain sizes and the modeling results indicate two different growth behaviors. Although the obtained kinetic parameters are suitable to describe grain growth behavior of these two groups, care is required when using them in a general sense because

several factors are not yet sufficiently understood: (1) How do second phases influence the growth kinetics (see also Covey-Crump 1997; Mas and Crowely 1996)? (2) What is the influence of fluids on grain growth in nature? (3) How representative are the kinetic parameters obtained in a more general sense? With a view to future work, therefore, more natural case studies with well-defined T–t paths and investigations on the type, quantity and distribution of impurities are required. In addition, the effect of impurities like porosity, chemical impurities and second phases needs to be addressed in laboratory experiments as well, to obtain well-constrained kinetic parameters which will allow a better extrapolation to nature.

Acknowledgements We gratefully acknowledge stimulating discussions with K. Ramseyer, X. Xiao and B. Evans. Special thanks go to the SEM facility (University of Basel) for providing access to their FEG and particularly to Marcel Düggelin for his introduction. This study would not have been possible without the samples provided by J. Schmid and the excellent sample separation performed by J. Megert and V. Jakob. We appreciated the careful reviews of the two journal referees Jörg Renner and Steven Covey-Crump and the proof reading of Monique Hobbs. M. Herwegh acknowledges financial support by SNF grant 21-66889.01.

References

Akinfiev N, Diamond WL (2002) Thermodynamic description of aqueous none-electrolytes at infinite dilution over a wide range of state properties. Geochem Cosmochim Acta 67:613–627

Brack P (1984) Multiple Intrusion—Examples from the Adamello Batholith and their significance of the mechanism of intrusion. Mem Soc Geol Ital 26:145–157

Brook RJ (1976) Controlled grain growth. In: Wang FFY (ed) Ceramic fabrication processes. Treatise on material science and technology, vol 9. Academic Press, New York, pp 331–364

Bucher K (1982) On the mechanism of contact aureole formation in dolomite country rock by the Adamello intrusion (N-Italy). Am Mineral 67:1101–1117

Burkhard M (1993) Calcite twins, their geometry, appearance and significance as stress-strain markers and indicators of tectonic regime: a review. J Struct Geol 15:351–369

Callegari E (1962) La Cima Uzza (Adamello Sud-Orientale) Part 1: Studio petrograficico e petrogenetico delle formazione metamorfiche di contatto. Mem Istit Geol Mineral Univ Padova 23:116

Callegari E, Dal Piaz G, Gatto GO (1999) Carta Geologica del Gruppo Adamello-Presanella

Chai BHT (1974) Mass transfer of calcite during hydrothermal recrystallization. In: Hofmann AW, Giletti BJ, Yoder HSJ, Yund RA (eds) Geochemical transport and kinetics, 634. Carnegie Inst of Washington, pp 205–218

Covey-Crump SJ (1986) Grain growth kinetics of calcite aggregates. MSc Thesis, University of London

Covey-Crump SJ (1997) The normal grain growth behavior of nominally pure calcitic aggregates. Contrib Mineral Petrol 129:239–254

Davidson C, Hollister L, Schmid S (1992) Role of melt in the formation of a deep-crustal compressive shear zone: The Maclaren glacier metamorphic belt, south central Alaska. Tectonics 11 348–359

Dresen G, Evans B, Olgaard DL (1998) Effect of quartz inclusions on plastic flow in marble. Geophys Res Lett 25:1245–1248

Evans B, Renner J, Hirth G (2001) A few remarks on the kinetics of static grain growth in rocks. Int. J Earth Sci (Geol Rundsch) 90:88–103

Exner HE (1972) Analysis of grain- and particle-size distributions in metallic materials. Int Metal Rev 17:25–42

Freund D, Rybacki E, Dresen G (2001) Effect of impurities on grain growth in synthetic calcite aggregates. Phys Chem Minerals 28:737–745

Gerdes ML, Baumgartner LP, Valley JW (1999) Stable isotopic evidence for limited fluid flow through dolomitic marble in the Adamello contact aureole, Cima Uzza, Italy. J Petrol 40:853–872

Hansmann W, Oberli F (1991) Zircon inheritance in an igneous rock suite of the southern Adamello batholith (Italian Alps): implication for petrogenesis. Contrib Mineral Petrol 107:501–518

Hanson RB (1995) The hydrodynamics of contact metamorphism. Geol Soc Am Bull 107:595–611

Hanson RB, Barton MD (1989) Thermal development of low-pressure metamorphic belts: Results from two dimensional numerical models. J Geophys Res 94:10363–10377

Herwegh M (2000) A new technique to automatically quantify microstructures of fine-grained carbonate mylonites: two step etching combined with SEM imaging and image analysis. J Struct Geol 22:391–400

Herwegh M, Kunze K (2002) The influence of nano-scale second phase particles on deformation of fine-grained calcite mylonites. J Struct Geol 24:1463–1478

Hillert M (1965) On the theory of normal and abnormal grain growth. Acta Metall 13:227–238

Jaeger JC (1964) Thermal effects of intrusions. Rev Geophys 2:44–54

Joesten RLJ (1983) Grain growth and grain boundary diffusion in quartz from Christmas Mountain (Texas) contact aureole. Am J Sci 283A:233–254

Joesten RLJ (1991) Kinetics of coarsening and diffusion-controlled mineral growth. In: Kerrick DM (ed) Contact metamorphism. Rev Mineral 26:507–582

Joesten RLJ, van Horn SR (1999) Numerical modeling of calcite coarsening in the aureoles of en echelon dikes: analysis of the kinetic control of isograd geometry in contact metamorphism. In: Jamtveit B, Meakin P (eds) Growth, dissolution and pattern formation in geosystems. Kluwer, Dordrecht, pp 109–141

Karato S, Masuda T (1989) Anisotropic grain growth in quartz aggregates under stress and its implication for foliation development. Geology 17:695–698

Mas DL, Crowley PD (1996) The effect of second-phase particles on stable grain size in regionally metamorphosed polyphase calcite marbles. J Metamorph Geol 14:155–162

Masuda T, Morikawa T, Nakayama Y (1997) Grain-boundary migration of quartz during annealing experiments at high temperatures and pressures, with implications for metamorphic geology. J Metamorph Geol 15:311–322

Matile L, Widmer T (1993) Kontaktmetamophose von kieseligen Dolomiten, Mergeln und Peliten im Südosten der Buffione Intrusion (SE Adamello, N-Italien). Schweiz Mineral Petrol Mitt 73:53–67

Nichols SJ, Mackwell SI (1991) Grain-growth in porous olivine aggregates. Phys Chem Mineral 18:269–278

Oertel G (1983) The relationship of strain and preferred orientation of phyllosilicate grains in rocks - a review. Tectonophysics 100:413–447

Olgaard DL, Evans B (1986) Effect of second-phase particles on grain growth in calcite. J Am Ceram Soc 69:C272–277

Olgaard DL, Evans B (1988) Grain growth in synthetic marbles with added mica and water. Contrib Mineral Petrol 100:246–260

Renner J, Evans B (2002) Do calcite rocks obey the power-law creep equation? In: de Meer S, Drury MR, de Bresser JHP, Pennock GM (eds) Deformation mechanisms, rheology and tectonics: current status and future perspectives. Geol Soc London, pp 293-307

Renner J, Evans B, Hirth G (2002) Grain growth and inclusion formation in partially molten carbonate rocks. Contrib Mineral Petrol 142:501–514

Riklin K (1983) Contact metamorphism of the Permian "red sandstone" in the Adamello area. Mem Soc Geol Ital 26:159–169

Schmid J (1997) The genesis of white marbles: geological cause and archaeological applications, p. 156. PhD Thesis, University Bern
Schmid J, Flammer I (2002) How gray limestones become white marbles. Eur J Mineral 14:837–848
Spry A (1969) Metamorphic textures. Pergamon Press, Oxford, 350 pp
Tullis J, Yund RA (1982) Grain growth kinetics of quartz and calcite aggregates. J Geol 90:301–318
Turcotte DL, Schubert G (2002) Geodynamics: Applications of continuum physics to geological problems. Wiley, New York, 450 pp
Walker AN, Rutter EH, Brodie KH (1990) Experimental study of grain-size sensitive flow of synthetic, hot pressed calcite rocks. In: Knipe RJ, Rutter EH (eds) Deformation mechanisms, rheology and tectonics, vol 54. Geological Society, Special Publication, pp 259–284